Multicomponent wavefield characterization with a novel scanning laser interferometer

Thomas E. Blum,[1,a)] Kasper van Wijk,[1] Bruno Pouet,[2] and Alexis Wartelle[2]
[1]*Department of Geosciences, Boise State University, 1910 University Drive, Boise, Idaho 83725, USA*
[2]*Bossa Nova Technologies LLC, 606 Venice Blvd., Suite B, Venice, California 90291, USA*

(Received 1 April 2010; accepted 24 May 2010; published online 6 July 2010)

The in-plane component of the wavefield provides valuable information about media properties from seismology to nondestructive testing. A new compact scanning laser ultrasonic interferometer collects light scattered away from the angle of incidence to provide the absolute ultrasonic displacement for both the out-of-plane and an in-plane components. This new system is tested by measuring the radial and vertical polarization of a Rayleigh wave in an aluminum half-space. The estimated amplitude ratio of the horizontal and vertical displacement agrees well with the theoretical value. The phase difference exhibits a small bias between the two components due to a slightly different frequency response between the two processing channels of the prototype electronic circuitry. © *2010 American Institute of Physics.* [doi:10.1063/1.3455213]

I. INTRODUCTION

Ultrasonic measurements have found application ranging from medical imaging and nondestructive testing to scaled modeling for seismology. Contacting piezoelectric transducers have traditionally been used as both source and receiver, but using these can result in mechanical ringing and variations in coupling. In addition, transducers are on the order of the size of the resonant wavelength, which can make them scatter the wavefield. Laser-based ultrasound has become an alternative noncontacting technique to transducers.[1] Ultrasonic laser interferometers and vibrometers have a broadband response and a submillimeter spot size. Since these laser-based sensors do not require physical coupling, one can scan a surface under computer control. Typically only the out-of-plane component of the wavefield is recorded, but Nishizawa *et al.*[2] performed two mutually orthogonal laser measurements at 45° incidence in addition to a normally incident measurement to get the in-plane component of the wavefield. Cand *et al.*,[3] on the other hand, used a two-channel confocal Fabry–Pérot interferometer and collected scattered light in two symmetrical directions with respect to the plane of normal incidence. Finally, Staszewski *et al.*[4] acquired two-dimensional scans of Lamb waves in metallic samples. Their costly system used includes three laser beam heads and involves extensive alignment with a location/range-finding geometry module; the alignment can be a limiting factor for spatial resolution, and therefore restricts this sensor to lower frequencies. Here, we present a novel single-beam adaptive interferometer to detect both the out-of-plane and the horizontal in-plane displacement components, on the fly. As an example, we describe calibration measurements of the Rayleigh wave in a large aluminum sample.

II. DESCRIPTION OF THE SENSOR

Our adaptive laser ultrasonic receiver is based on a constant-wave doubled Nd:YAG (Neodymium-doped Yttrium Aluminum Garnet) laser, generating a stable 250 mW beam at a wavelength of 532 nm. The beam is split into a probe beam which is reflected by the sample surface and a reference beam which follows a fixed optical path inside the device. The receiver uses two-wave mixing in a photorefractive crystal to deliver the true displacement of the sample surface. The reference and object beams are combined in the photorefractive crystal to form a real-time hologram which diffracts each beam into the other direction. The crystal performs several critical functions. First, it acts as an adaptive beam splitter, which combines the transmitted signal beam with the diffracted reference beam with exact wavefront matching. Second, it compensates for slow variations in the wavefront of the signal beam. A DC voltage is applied to the crystal to enhance the grating diffraction efficiency and to provide the proper phase for coherent detection.

The optical setup is shown in Fig. 1. We take advantage of the roughness of the material surface by collecting the light scattered away from the angle of incidence (the *f*-number of the system is 0.8), which carries information on

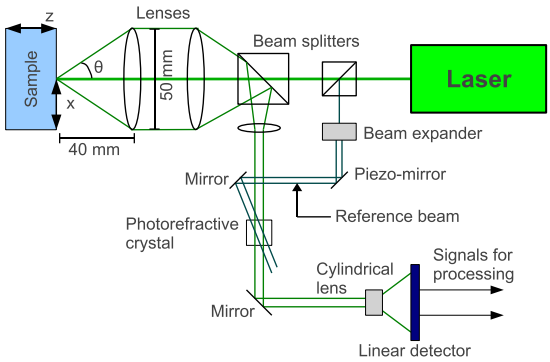

FIG. 1. (Color online) A diagram of the optical setup.

a)Electronic mail: tblum@cgiss.boisestate.edu.

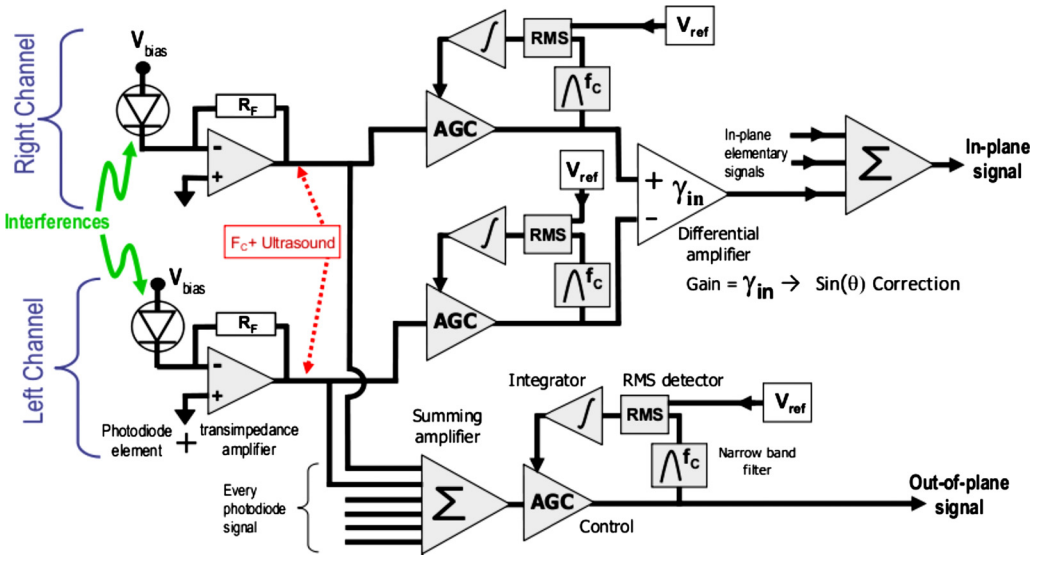

FIG. 2. (Color online) Electronic processing of the photodiode signal leading to the in-plane and out-of-plane output.

the in-plane displacement. After the reference and probe wavefront interfere in the photorefractive crystal, the circular beam goes through a cylindrical lens and is imaged on a linear 16-element photodiode. The optical setup is symmetric, so that elements can be treated in pairs corresponding to the same absolute angle. We number the elements $e_{\pm i}$ with $i=1$ for the center pair and $i=8$ for the outside pair; positive-numbered elements belong to one-half of the photodiode and negative-numbered elements to the other. Each detector element corresponds to an angle θ_i at which the collected light is scattered by the sample surface. Since out-of-plane motion is symmetric with respect to the probe beam axis, but in-plane motion is asymmetric, the motion recorded by the element e_i is $s_{\pm i}=\cos(\theta_i)u_z \pm \sin(\theta_i)u_x$, where u_z and u_x are the displacements along the (out-of-plane) z axis and (horizontal in-plane) x axis.

For small angles θ_i, we find that

$$u_z = (s_i + s_{-i})/[2\cos(\theta_i)] \approx (s_i + s_{-i})/2,$$

$$u_x = (s_i - s_{-i})/[2\sin(\theta_i)] \approx (s_i - s_{-i})/2\theta_i.$$

As a result, the out-of-plane displacement is obtained by summing over all elements, but for the in-plane motion each element pair is treated with an automatic gain control and a differential amplifier proportional to $1/\theta_i$, as shown in Fig. 2, before the resulting signals are summed together.

To calibrate the measured particle displacements, a piezoelectric transducer mounted with a mirror introduces a known displacement at a low frequency f_c on the reference beam. This signal is bandpass filtered and feeds an amplification loop controlled by the reference voltage V_{ref} to calibrate the in-plane and out-of-plane signals at 100 mV/nm.

III. POINT MEASUREMENT

We measure the amplitude and phase of a Rayleigh wave in an aluminum block ($214\times232\times277$ mm^3) previously described in Scales and van Wijk[5,6] and van Wijk *et al.*[7,8] Elastic waves are generated by a pulsed Nd:YAG laser source, with a 20 Hz repetition rate. The source beam is partially focused, resulting in a circular source spot approximately 4 mm in diameter, 77 mm from the receiver (Fig. 3). The in-plane and out-of-plane signal are averaged 500 times, and then bandpass filtered between 300 and 900 kHz, so that

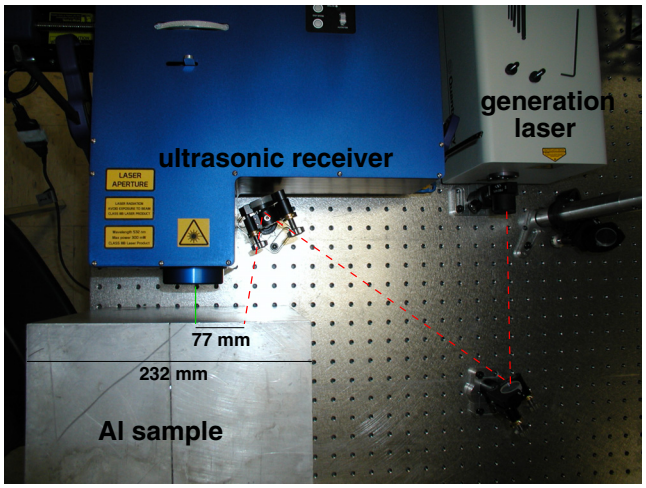

FIG. 3. (Color online) Top view of the experimental setup with the generation beam represented by a dashed line and the receiver beam by a solid line.

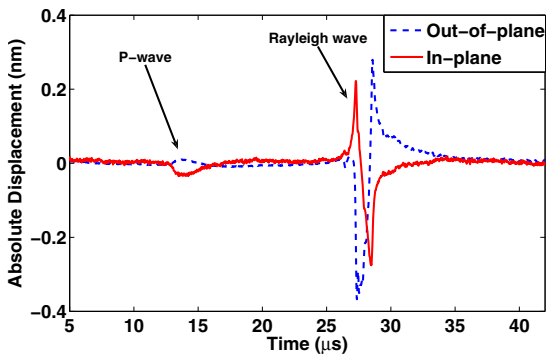

FIG. 4. (Color online) Unfiltered signal recorded by the interferometer 77 mm away from the source. Positive values are radially outward and up.

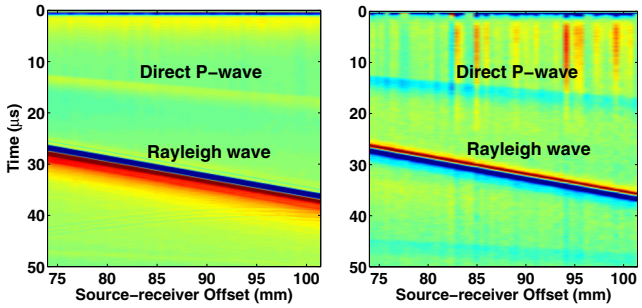

FIG. 5. (Color online) Line scan for the out-of-plane component (left) and the in-plane component (right).

all edges of the sample as well as the source spot are tens of wavelengths away. We therefore consider the detection to be in the far field, where the wave modes are fully established. The Rayleigh wave in this effectively homogeneous isotropic half-space is characterized by elliptical retrograde motion at the free surface: the horizontal and vertical components of the displacement are 90° out of phase. Furthermore, the ratio between the maximum amplitudes of the two components (the so-called H/V ratio) is $2\sqrt{1-c_x^2/\beta^2}/(2-c_x^2/\beta^2)$, where β is the shear wave velocity and c_x the Rayleigh wave velocity.[9,10] Based on our data and previous studies in this sample, $\alpha=6060$ m/s, $\beta=3120$ m/s, and $c_x=2905$ m/s, resulting in an H/V ratio of 0.64.

The absolute displacements from both channels are presented in Fig. 4. We estimate the H/V ratio to be 0.64 ± 0.02 from the discrete amplitudes in the power spectrum and obtain the phase difference by subtracting the unwrapped phase angles of the complex part of the Fourier transform, similarly to Cand *et al.*[3] However, we find the phase difference between the in-plane and out-of-plane wavefields to be $97\pm1°$, a bias of 7°. All error bars represent the uncertainty at 2σ, where σ is the standard deviation in the phase and amplitude calculation over all frequencies, respectively. The most significant source of error in our H/V estimates is due to the in-plane signal, as shown in Fig. 7. This phase offset originates from a difference in the frequency response between the electronic circuitry for calculation of the in-plane and out-of-plane signals, as explained in Sec. II. In the future, the phase difference can be eliminated by carefully matching the frequency response of both in-plane and out-of-plane circuits.

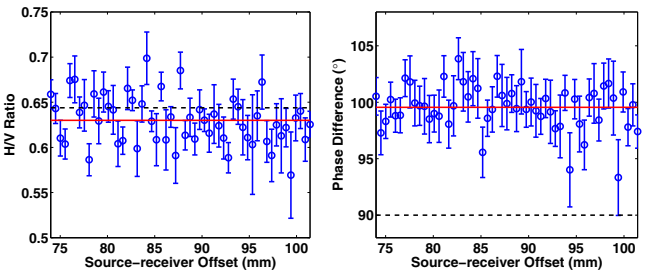

FIG. 6. (Color online) Amplitude ratio (left) and phase difference (right) as a function of source-detector offset. The average and theoretical values are plotted as dashed and solid lines, respectively.

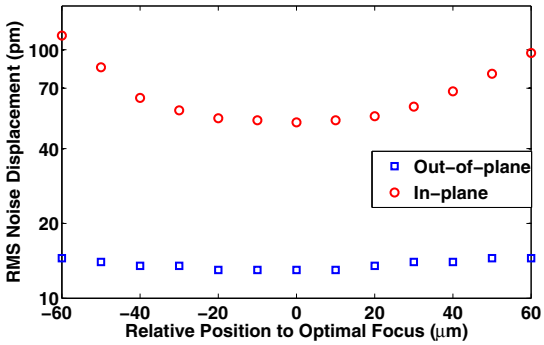

FIG. 7. (Color online) rms noise displacement (in picometer) measured on the in-plane and out-of-plane channels as the beam looses focus. The RMS value is taken over the 0–20 MHz bandwidth.

IV. A PRELIMINARY LINE SCAN

We place the receiver on a motorized stage to record the ultrasonic signals at source-detector offsets between 74 and 101 mm, acquired every half millimeter (Fig. 5). Once we focus the beam in the center of the acquisition line, the entire scan is automatic and lasts on the order of minutes. Figure 6 displays an average H/V ratio of 0.63 ± 0.05 and a phase difference of $100\pm4°$. We attribute variations in the scan results to small variations in detector focus cause by a variable distance to the sample on the order of tens of micrometers. Because a large collecting angle is required for good in-plane sensitivity, it is critical to be well positioned at the focus in order to achieve accurate in-plane measurement. Figure 7 shows how quickly the in-plane noise level increases, and therefore the signal-to-noise ratio degrades, when moving out of focus. The focus positioning accuracy is not as critical for the out-of-plane detection. Future work involves the development of an autofocusing module in order to maintain the focus position corresponding to the lowest in-plane noise level, as shown in Fig. 7, and obtain the highest accuracy in phase and amplitude in automated scans.

V. CONCLUSION

A new laser interferometer takes advantage of the surface roughness of the sample for light to scatter away from the angle of the incident laser beam. The reflected light is recorded on a linear array of photodiodes, after which in-plane and out-of-plane particle displacements are determined. First results indicate that the amplitudes match theoretical calculations. The phase information is slightly biased because of a difference in the frequency response of electronic circuitry to measure in-plane and out-of-plane motions. The sensor allows for rapid scanning of the wavefield; future implementation of an autofocus module based on monitoring the noise level of the in-plane signal should further improve accuracy of the scanned wavefield.

ACKNOWLEDGMENTS

The development of the sensor was funded by the NSF Grant No. IIP-0712620. T.B. and K.v.W. thank ConocoPhillips for their support of this research.

[1] C. B. Scruby and L. E. Drain, *Laser Ultrasonics Techniques and Applications*, 1st ed. (Taylor & Francis, London, 1990), p. 462.
[2] O. Nishizawa, T. Satoh, and X. Lei, Rev. Sci. Instrum. **69**, 2572 (1998).
[3] A. Cand, J.-P. Monchalin, and X. Jia, Appl. Phys. Lett. **64**, 414 (1994).
[4] W. J. Staszewski, B. C. Lee, and R. Traynor, Meas. Sci. Technol. **18**, 727 (2007).
[5] J. A. Scales and K. van Wijk, Appl. Phys. Lett. **74**, 3899 (1999).
[6] J. A. Scales and K. van Wijk, Appl. Phys. Lett. **79**, 2294 (2001).
[7] K. van Wijk, M. Haney, and J. A. Scales, Phys. Rev. E **69**, 036611 (2004).
[8] K. van Wijk, D. Komatitsch, J. A. Scales, and J. Tromp, J. Acoust. Soc. Am. **115**, 1006 (2004).
[9] P. G. Malischewsky and F. Scherbaum, Wave Motion **40**, 57 (2004).
[10] S. Stein and M. Wysession, *An Introduction to Seismology, Earthquakes, and Earth Structure*, 1st ed. (Wiley-Blackwell, Malden, MA, 2002).